

Effect of Distributor Plate Configuration on Pressure Drop in a Bubbling Fluidized Bed Reactor

A.E. Ghaly^{1*}, A. Ergudenler² and V. V. Ramakrishnan¹

¹Department of Process Engineering and Applied Science Department,
Faculty of Engineering, Dalhousie University,
Halifax, Nova Scotia, Canada

ABSTRACT

Aim: To study the effects of distributor plate shape and conical angle on the pressure drop were studied in a pilot scale fluidized bed system.

Methodology: Five distributor plates (flat, concave with 5°, concave with 10°, convex with 5° and convex with 10°) were used in the study. The system was tested at two levels of sand particle size (a fine sand of 198 µm and coarse sand of 536 µm), various bed heights (0.5 D, 1.0 D, 1.5 D and 2.0 D cm) and various fluidization velocities (1.25, 1.50, 1.75 and 2.00 U_{mf}).

Results: The pressure drop was affected by the shape and the conical angle of distributor plate, sand particle size and bed height. Less than theoretical values of the pressure drop were observed with the 10° concave distributor plate at lower fluidizing gas velocities for all bed heights. A decrease in the angle of convex and an increase in the angle of concave resulted in a decreased pressure drop. Greater values of pressure drop were obtained with larger sand particles than those obtained with small sand particles at all fluidizing velocities and bed heights. For all distributor plates, increasing the bed height increased the pressure drop but decreased the ratio of pressure drop across the distributor to the pressure drop across the bed (Δ_{PD}/Δ_{PB}). There was no variation in the pressure drop in the freeboard.

Conclusion: Fluidizing gas velocities higher than 1.25 U_{mf} should be used to for a better fluidization, improved mixing and avoiding slugging of the bed.

Keywords: Fluidized bed, pressure drop, fluidization velocity, particle size, bed height, distributor plate, concave, convex, angle, location

1. INTRODUCTION

Cereal straws have come in recent years to be regarded as an unwanted companion of the cereal crops. Their use as animal feedstuff, livestock bedding materials, erosion control agents, building materials, chemical sources, pulping material and craftwork materials have diminished [1]. These residues can be better utilized by converting them directly to energy (by combustion) or to energy carrying products (by gasification, pyrolysis and fermentation). These products could be used to meet farm energy needs or be transported for use of farm [2]. The organic carbon formed within the biomass during photosynthesis is released during combustion of biomass (or biofuels driven from biomass), making biomass a carbon neutral energy source [3, 4]. The conversion of biomass into usable energy sources represents a vital method of reducing fossil fuel dependence and greenhouse gas emission. The low

* Tel.: +1-902-494-6014; fax: +1-902-423-7639
E-mail address: abdel.ghaly@dal.ca.

levels of impurities in biomass lead to lower SO_x and NO_x emission during combustion and thus reduced contribution to acid rain [5].

Gasification as a thermochemical conversion process can be used to convert cereal straws into syngas. One of the important features of gasification of cereal straws is that the reaction temperature can be kept as low as 600°C, thereby preventing sintering and agglomeration of the ash which occurs during the high temperature (100-1200°C) of the combustion process [6]. Fluidized bed reactors have been shown to be more suitable than moving or fixed bed reactors for the gasification of low density fuels such as crop residues because they are less prone to slagging.

The application of fluidized bed gasification technology to cereal straw is increasing rapidly [7, 8]. Effective gasification of straw requires rapid mixing of the fuel material with the inert sand of the bed in order to obtain a uniform distribution of the fuel particles, a better chemical conversion and a uniform temperature throughout the bed [9-10,3]. However, mixing problems in fluidized bed systems become very severe when fuel particles vary both in size and density resulting in material segregation [7, 11-12]. One of the main causes of segregation is the out of balance forces during the periodic disturbances with the passage of the bubbles due to differences in density [12].

The gas distributor plate is one of the most critical features in the design of a fluidized bed reactor [7]. The use of a suitable gas distributor is essential for satisfactory performance of gas-solid fluidized beds [13]. Understanding of solids mixing and flow characteristics of gases and solids near the grid region of a fluidized bed reactor is vitally important from the standpoint of design and scale up of gas distribution systems [14]. The presence of stagnant zones near grid region can cause hot spots resulting in agglomeration and eventual reactor failure [6]. Ghaly and MacDonald [13] developed a concave/convex type distributor plate which provided good mixing characteristics and a complete bed material turnover that prevented the occurrence of stagnant zones near the grid region.

The pressure drop across the bed is another important factor to consider when designing a fluidized bed gasification system. The quality of fluidization taking place in the bed can be deduced from the bed pressure drop. Theoretically, the pressure drop across the bed should be equal to the weight of the bed particles per unit cross-sectional area of the fluidizing column as follows [15, 16]:

$$\Delta P = \frac{W}{A} \quad (1)$$

The weight of the bed particles (W) is calculated as follows:

$$W = H A (\rho_p - \rho_g)(1 - \epsilon_{mf}) \quad (2)$$

Equations 1 and 2 can be combined as follows:

$$\Delta P = H (\rho_p - \rho_g)(1 - \epsilon_{mf}) \quad (3)$$

Where:

ΔP	=	Pressure drop (kPa)
W	=	Weight (g)
A	=	Cross sectional area (cm ²)
g	=	Gravitational constant (9.8 cm/s ²)
H	=	Height of fixed bed (cm)
ρ_p	=	Density of the particle (g/cm ³)

85 ρ_g = Density of fluidizing gas (g/cm³)
 86 ϵ_{mf} = Bed voidage at minimum fluidization (-)
 87

88 However, several studies showed that the pressure drop across the fluidized bed is slightly
 89 larger than the weight of the bed particles per unit cross-sectional area [17, 18]. These
 90 authors indicated that both experimental and calculated pressure drops were smaller than
 91 the value estimated from the gravity of the particles because the particles present do not
 92 fluidize uniformly. Menon and Durian [17] reported that the pressure drop across the
 93 fluidized bed reactor is normalized by the weight of the entire bed per unit area. Taghipour et
 94 al. [18] reported that the overall bed pressure drop decreased significantly at the beginning
 95 of fluidization and fluctuated around steady state due to bubbles being continuously split and
 96 coalesce in a transient. Kawaguchi et al. [19] reported that there will be strong pressure
 97 fluctuations when bubbling and slugging occurs is estimated from the gravity of the particles
 98 because the particles present do not fluidize uniformly.
 99

100 Pressure drop fluctuations have been observed in gas fluidized beds is a good method
 101 determining fluidization quality. Large fluctuations may indicate slugging and no fluctuations
 102 at all may indicate severe channeling in the bed. Moderate fluctuations indicate good
 103 fluidization. Therefore, for a good gas particles distribution, distribution plates are designed
 104 such that gas passing a through them experience sufficient pressure drop to prevent the
 105 formation of channels in the bed. Geldart and Beayens [20] have shown that the pressure
 106 drop (ΔP) across a distributor plate can be calculated as follows:
 107

$$\Delta P_d = \frac{\rho_g U^2}{2 C_d^2 F^2} \quad (4)$$

108 Where:

109 ΔP_d = Pressure drop across distributor plate (kPa)
 110 ρ_g = Density of fluidizing gas (g/cm³)
 111 U = Fluidizing gas velocity (cm/s)
 112 C_d = Discharge coefficient (-)
 113 F = Fractional free area (-)
 114
 115

116 The discharge coefficient (C_d) depends on the shape of the plate orifice (hole) fractional free
 117 area (F). Also, the thickness of the plate affects the discharge coefficient and hence the
 118 pressure drop. The thicker the distributor plate, the lower the pressure drop across the plate
 119 [21]. Clift [22] showed that for square-edged circular orifice with diameter (d_o) much larger
 120 than the plate thickness (t_p), C_d can be taken as 0.6 for t_p/d_o greater than 0.09. Qureshi and
 121 Creasy [21] gave the following correlation between C_d and t_p/d_o :
 122

$$C_d = 0.82 \left[\frac{t_p}{d_o} \right]^{0.13} \quad (5)$$

124 Where:

125 d_o = Orifice diameter (cm)
 126 t_p = Plate thickness (cm)
 127
 128

129 The pressure drop across the distributor plate can be calculated as a function of the bed
 130 pressure drop and aspect ratio using the following correlation [21]
 131

$$\frac{\Delta P_D}{\Delta P_B} = 0.01 + 0.2 \left[1 - \exp \left(-0.5 \frac{D}{H_{mf}} \right) \right] \quad (6)$$

Where:
 D = Bed diameter (cm)
 H_{mf} = Bed height at minimum fluidization (cm)
 ΔP_d = Pressure drop across distributor plate (kPa)
 ΔP_b = Bed pressure (kPa)

Pressure drop across the distributor plate can be used to deduce information regarding solids circulation patterns and to show whether the performance of the plate is changing with time or not. The main aim of the study was to investigate the effects of distributor plates configuration (shape and angle) on pressure drop in a bubbling fluidized bed gasification system operating at room temperature and various levels of sand particle size, bed height and fluidization velocity.

2. EXPERIMENTAL APPARATUS

The experimental apparatus used in this study is shown in Figure 1. The system consisted of: (a) a fluidized bed reactor, (b) an air supply unit, (c) a cyclone and (d) a pressure drop measurement system. With reference to Figure 1, the following are detailed descriptions of the system components.

2.1. Fluidized Bed Reactor

The fluidized bed reactor consisted of: (a) a support stand, (b) a conical inlet section, (c) a distributor plate, (d) a fluidizing column, (e) a disengagement section and (f) an outlet duct.

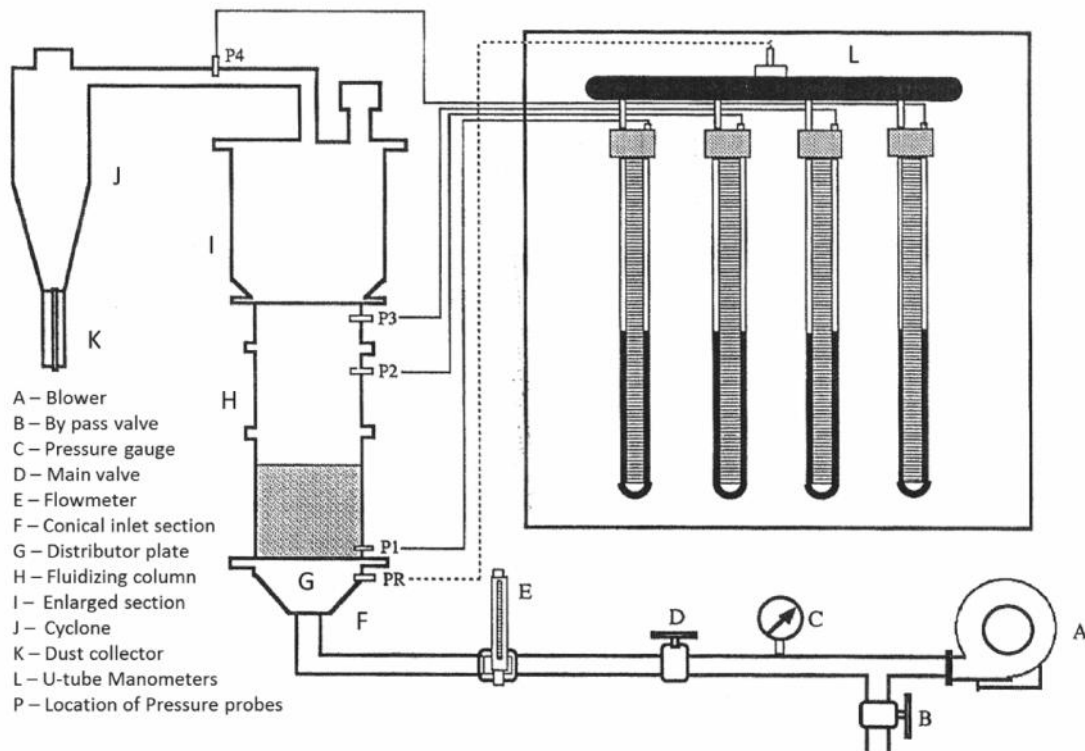
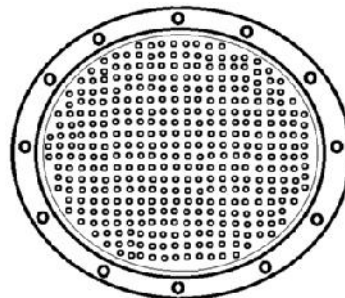


Fig. 1. Experimental Apparatus.

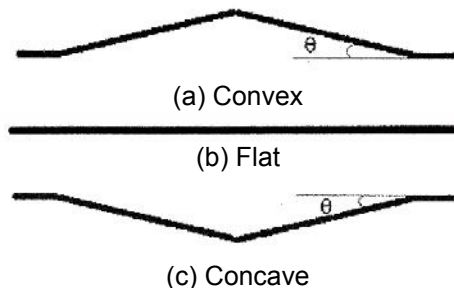
161 The support stand was constructed of 3.8 cm steel angle iron. A horizontal square structure
 162 made of four 38 cm long angle iron arc welded together was supported by four 47/5 cm long
 163 legs. These were arc welded to the corners of the square structure. The legs were inclined at
 164 15° from vertical for stability; thereby giving a stand floor base of 52.5 cm x 52.5 cm. The
 165 total height of the support stand was 46 cm. At the middle of each side of the square
 166 structure, a .06 cm thick L-shaped steel extension was welded in a vertical position so that
 167 the flange of the conical inlet section of the fluidized bed reactor could lay on these
 168 extensions. Four 0.8 cm x 3.0 cm hex head bolts were used to fix the inlet section to the
 169 support stand.

170
 171 The vertical section of the airline was connected to a conical (funnel shaped) inlet section
 172 made of 0.32 mm thick stainless steel material. The height of the conical section was 12 cm.
 173 Its sides were inclined at 45° from vertical. The bottom and top diameters of the conical
 174 section were 6/3 cm and 25.5 cm, respectively. A flange (collar) made of 0.8 cm thick
 175 stainless steel was welded to the upper portion of the funnel. The inner and outer diameters
 176 of the flange were 25.5 cm and 35.5 cm, respectively. A thick rubber gasket of 0.3 mm
 177 thickness was used between the flanges of the conical inlet section and the distributor plate
 178 to provide good sealing.

179
 180 The distributor plate was made of 0.8 mm thick circular steel plate of 35.5 cm diameter. A
 181 circular area of 22 cm diameter was perforated. The total open area of the holes was 1.63%
 182 of the bed cross-sectional area. A total of 267 holes of 0.2 cm diameter each were drilled in
 183 the circular plate in the form of rings starting from the center with a pitch of 1.11 cm. To
 184 prevent falling of the sand through the holes of the distributor plate, a circular screen of 100
 185 mesh size was point welded to the top of the distributor plate. Five plates having exactly the
 186 same open area and same number of vertical holes were manufactured (10° concave, 5°
 187 concave, flat, 5° convex and 10° convex) and used to test the effect of distributor plate
 188 configuration on the pressure drop in the fluidized bed (Figure 2).
 189



Hole diameter = 0.2 cm
 Number of holes = 267
 Perforated area = 1.63%
 $\Theta = 0^\circ, 5^\circ, 10^\circ$



199
 200
 201 **Fig. 2. Type of distributor plates.**

The main body of the fluidized bed (fluidizing column) was made of a Plexiglas cylinder having 25.5 cm inside diameter and 5 mm thickness. It was constructed in three pieces having lengths of 12.75, 25.5, 38.25 cm (0.5, 1.0, 1.5 D), respectively. This provided a maximum height of 76.5 cm. Two flanges made of 0.8 cm thick circular plates were glued to the top and bottom of each cylinder. The height of the fluidizing column was varied by fitting different sections of varying lengths. The sections were bolted to each other and rubber type O-rings of 0.3 cm thickness were used between them to provide good sealing. A 5.5 cm diameter port was provided near the bottom of the bed to remove the bed material when required.

To decrease the rate of elutriation from the top of the fluidized bed, an enlarged section was used at the upper part of the bed. This part was made from 0.2 cm thick, hot rolled steel. The sides were inclined at 30° from vertical. The bottom and top diameters were 25.5 cm and 35 cm, respectively. The total height of this enlarged section, including the inclined part, was 39.5 cm. The top of this enlarged section was covered with 6 mm thick hot rolled steel, which was connected to the outlet duct.

The outlet duct was made of 0.16 cm thick stainless steel material. The vertical section of the duct was 10 cm in length whereas the horizontal section of the duct was 40 cm in length. The vertical section of the duct had a cross-section of 8.5 mm x 8.5 cm at the bed exit whereas the horizontal section has a cross section of 8 mm x 4 cm at the cyclone inlet.

2.2. Air Supply

The air supply system consisted of: (a) a blower equipped with a filter, (b) a pressure gauge, (c) a main valve, (d) a by-pass valve, (e) an air line and (f) a flow meter. A blower (Model Engenair R43 1 OA-2-220 volts and 1 3/4 amps Benton Harbour, MI, USA) having a maximum flow rate of 81.2 L/s was used. The blower was powered by a 4.8 hp, 3 phase electric motor (Blador Industrial motor, 5711, Fort Smith, Arizona, USA) and ran at a speed of 2850 rpm. The maximum pressure that can be obtained from the blower was 212 cm H₂O (2.08 kPa). A filter having a pore size of 25 µm and a maximum flow of 7080 L/min was used at the blower inlet to filter the incoming air in order to supply dust and water free air to the fluidized bed reactor. The airline, through which the air was supplied to the fluidized bed, was composed of horizontal and vertical steel pipe sections. The horizontal section on which the flow meter and main valve were mounted was connected to a 60 cm long horizontal steel pipe having an inner diameter of 6.3 cm. This was connected to a 10 cm long vertical pipe by a 90° elbow having the same inner diameter. The bypass valve was located on the vertical pipe. A pressure gauge (USG) having a pressure range of 0-690 kPa with a scale of 13.8 kPa increments was used at the exit of the blower to check the pressure level in the air supply line in order to maintain atmospheric pressure in the bed. The main valve was used to control the air flow rate while the by-pass valve was used to by-pass the excess air to avoid over heating of the motor.

The flow rate of the fluidizing air was measured using Flow Cell Bypass Flow meter (a FLT type Cole Parmer Catalog No. N03251-60, Chicago, IL). This flow meter is accurate to 2.5 percent of full scale and can be used up to maximum temperature and pressure of 60 °C and 1035 kPa, respectively. Three flow meters (with different ranges 2.4-11.8, 5.6-25.5 and 11.8-52.1 L/s) were used depending on the required air flow rate. Each flow meter was installed in a horizontal pipe having the same flow meter size rating. The length of the pipe section downstream the flow meter was kept greater than three times the diameter of the pipe whereas that upstream the flow meter (after the valve) was greater than eight times the diameter of the pipe.

2.3. Cyclone

A cyclone connected to the outlet duct was used to capture the fine solid particles escaping from the top of the bed. The cyclone was made from a 0.2 cm thick stainless steel metal sheet. It consisted of a conical and a cylindrical section. The cylindrical section had a 150 mm diameter and a 30 cm height. The conical section had a 30 cm height and its sides were inclined at 60° from the vertical. A gas outlet pipe of 7.5 cm diameter was extended 9 cm axially into the cyclone. At the bottom of the cyclone, the fine dust particles were collected in a cylindrical Plexiglas dust collector of a 6 cm diameter and a 20 cm height.

2.4. Pressure Drop Measurement System.

The pressure drop was measured at different heights of the fluidized bed using vertically mounted U-tube manometers. The first measurement point was located in the bed (5 cm above the distributor plate) was used to measure the pressure drop across the distributor plate. The second and third measurement points were located in the freeboard, 60 and 72 cm above the distributor plate, respectively. The fourth measurement point was located on the outlet duct, connecting the bed exit to the cyclone. All of these pressure measurements were done with respect to a reference point located at the conical inlet section (5 cm below the distributor plate). All five U-tubes were mounted on a vertical plate. Colored water was used as the manometer liquid. Each measurement point was connected to a different U-tube using flexible, tygon tubing of 10 mm diameter. The other end of the U-tube was connected to the reference point through a manifold.

3. EXPERIMENTAL PROCEDURE

3.1. Experimental Design

In this study, the effects of 5 parameters on the pressure drop were investigated. The experimental parameters are shown in Table 1. These were: (a) pressure drop location, with 4 levels, (b) type of distributor plate, with 5 levels, (c) sand mean particle size, with two levels, (d) bed height, with 4 levels and (e) fluidizing velocity, with 4 levels. Three measurements were taken during each experimental run.

3.2. Determination of Particle Size

Two types of sand were used in the study: fine and coarse. The most common method used to measure the size of irregular particles larger than 75 μm is sieving [23]. Sieving operation was performed for both types of the sand used in the experiments. After sieving the mean size of the particles was determined using the following equation:

$$d_p = \frac{1}{\sum \frac{x_i}{d_{pi}}} \quad (7)$$

Where:

d = Mean size of the particles (cm)

x_i = Weight fraction of powder of size (-)

d_{pi} = Mean sieve size of a powder (cm)

The particle size distributions of the fine and coarse sands are given in Table 2 and represented in Figure 3.

305 **Table 1. Experimental parameters**
306

1. Distributor Plate				
Hole diameter (cm)	d_{or}	=	0.2	
Pitch (cm)	p	=	1.12	
Percent perforated area (%)	f_A	=	1.647	
Plate angle (°)	θ	=	5° concave, 10° concave, flat, 5° convex and 10° convex	
2. Sand Particle Size				
			Fine	Coarse
Mean diameter, d_p (cm)			0.0198	0.0536
Particle density ρ_p (g/cm ³)			2.6	2.6
Minimum fluidization velocity, U_{mf} (cm/sec)			4.2	26.0
3. Bed Height				
Column inner diameter (cm)	D	=	25.50	
Freeboard height (cm)	FB	=	50.00	
Disengagement height (cm)	DE	=	39.50	
Packed bed height (cm)	H	=	0.5 D, 1.0 D, 1.5 D, 2.0 D	
4. Fluidizing velocity (FV)				
Fluidizing gas	Air			
Room temperature (°C)	20-22			
Fluidization velocity (cm/s)	U_o	=	1.25 U_{mf} , 1.50 U_{mf} , 1.75 U_{mf} , 2.00 U_{mf} ,	
5. Pressure Drop Locations (XX)				
Reference point under distributor plate			5 cm	
Measurement location above distributor plate			5 cm, 60 cm, 72 cm, 132 cm	

307
308 **Table 2. Sand particle size.**
309

Sieve aperture (cm)		d_{pi} (cm)	Weight fraction (%)	
Minimum	Maximum		Fine	Coarse
850	0.1410	0.1130	0.00	0.77
595	0.0850	0.0723	1.28	34.50
425	0.0595	0.0510	19.95	57.40
297	0.0425	0.0631	23.36	5.85
212	0.0297	0.0254	22.57	0.82
0	0.0212	0.0106	32.84	0.66

310 d_p = Mean particle size (cm)
311 d_{pi} = Mean sieve size (cm)
312 d_p for fine sand = 0.0198 cm
313 d_p for coarse sand = 0.0536 cm
314

315 3.3. Determination of Pressure Drop across the Distributor Plate

316 The pressure drop across the distributor plate (PD) was taken to be 10% of the pressure
317 drop across the bed (PB). The pressure drop across the bed (PB) was determined from
318 Equation 2. Reynolds number for the total flow approaching the plate was calculated and the
319 corresponding value for the orifice coefficient (Cd) was selected according to the procedure

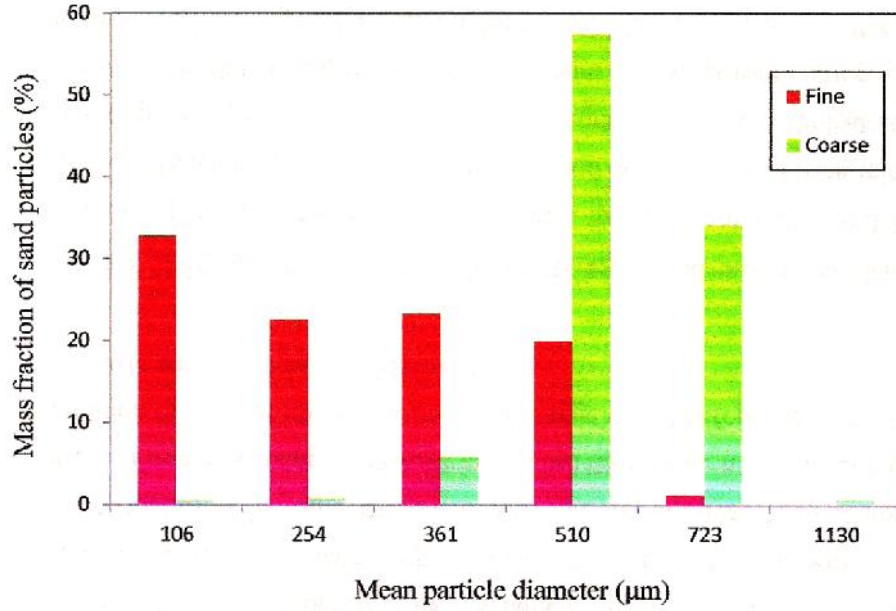


Fig. 3. Sand particle distribution.

described by Kunii and Levenspiel [24]. The velocity of fluid through the orifices (U_o) was determined as follows:

$$U_o = C_d \frac{0.5}{\rho_g} \quad (8)$$

Where:

- U_o = Gas velocity through the orifices (cm/s)
- P_D = Pressure drop across the distributor (KPa)
- C_d = Discharge coefficient (-)

The fraction of open area was found from the ratio U_o/U_s . Deciding on the orifice diameter (d_o), the corresponding number of orifices per unit area of distributor plate (N_{or}) was determined as follows.

$$N_{or} = \frac{4U_s}{\pi(d_{or})^2 U_o} \quad (9)$$

Where:

- N_{or} = Number of orifices per unit area (-)
- d_o = Diameter of the orifice (cm)
- U_s = Superficial gas velocity (cm/s)

3.4. Determination of the minimum fluidization velocity

The minimum fluidizing velocity was calculated using the following equation [25]:

$$U_{mf} = \frac{\mu_g}{\rho_p d_p} [C_1^2 + C_2 Ar]^{0.5} - C_1 \quad (10)$$

Where:

- μ_g = Viscosity of the fluidizing gas (g/cm s)
- ρ_g = Density of fluidizing gas (g/cm³)

351 ρ_p = Density of fluidizing gas (g/cm³)
352 $C_1 = 27.2$
353 $C_2 = 0.04086$
354

355 Archimedes number (A_r) can be calculated as follows [26]

356
$$A_r = \frac{\rho_g d_p^3 (\rho_p - \rho_g) g}{\mu_g^2} \quad (11)$$

357 **3.5. Experimental Protocol**

358
359 The Selected distributor plate was fixed in place and the fluidizing column was assembled.
360 One type of sand (fine sand) was then added to the reactor up to the required bed height.
361 The blower was turned on and the flow rate was adjusted until the required fluidizing velocity
362 was obtained. The pressure differences measured at various points above the distributor
363 plate was recorded. This was then repeated 3 times with a ten minute time interval between
364 measurements. The air flow rate was then changed and the procedure was repeat until three
365 measurements were taken for each of the flow rates.

366
367 More sand was then added to the desired bed height and the same procedure was followed
368 until three measurements were obtained for all bed height-flow rate combinations. The sand
369 was changed (course sand) and the above experiments were repeated as with the other
370 type (fine sand) of sand. Finally, the distributor plate was changed and all the above
371 experiments were repeated with all distributor plates.

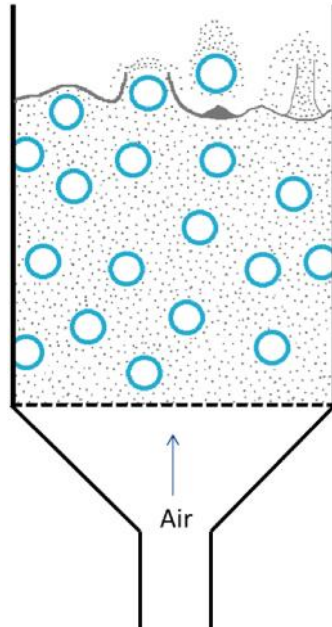
372 **4. RESULTS AND DISCUSSION**

373
374
375 The effect of the shape and angle of distributor plate on the pressure drop in a bubbling
376 fluidized bed reactor was investigated at various levels of sand particle size, bed height and
377 fluidizing velocity. The pressure drop was measured at four locations in the reactor. Three
378 pressure drop measurements were taken for each treatment combination.

379
380 The analysis of the high speed films indicated that vertical transport and mixing of particles
381 were achieved by bubble motion as each bubble carried a wake of particles that was
382 ultimately deposited on the bed surface (Figure 4). It caused a drift of particles to be drawn
383 up as a spout below it as it left the bed of sand. Muller et al. [27] used particle image
384 velocimetry to capture the radial mixing that occurs during bubble burst as shown in Figure
385 5. When the bubble rises to the surface, the bubble roof breaks down and the bubble erupts.
386 The bubble wake is ejected from the surface and then falls. The surface appears settled till
387 another bubble erupts.

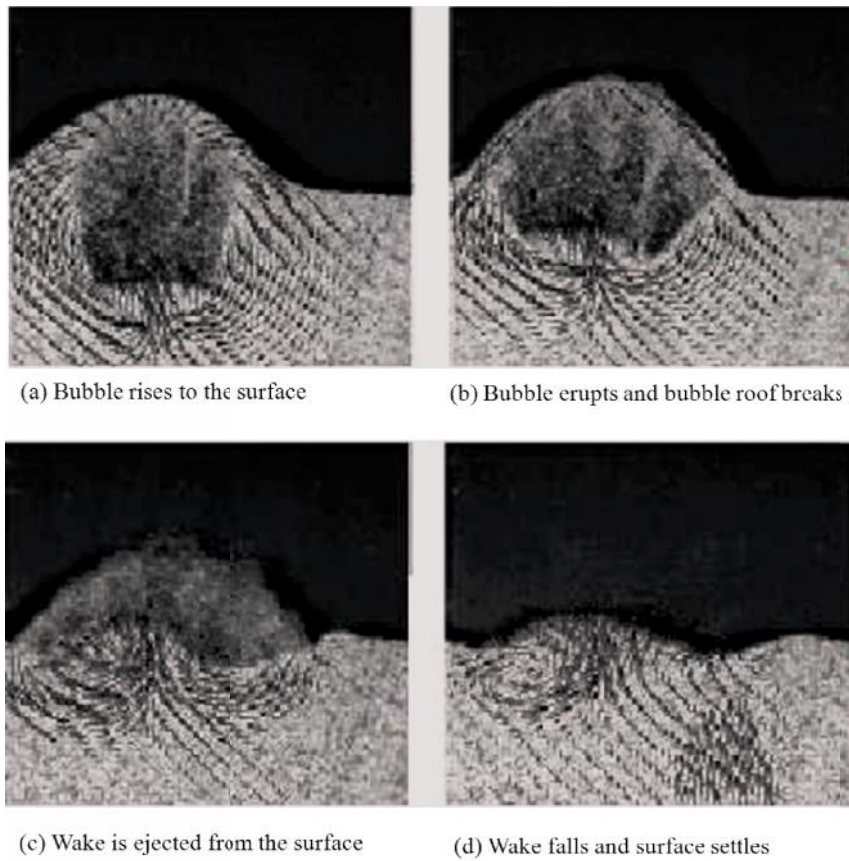
388
389 The shape (concave, convex or flat) and the angle of the distributor affected the vertical and
390 localized mixing as well as the upward/downward movement of sand particles (Figure 6).
391 With the concave distributor plate, there was an observed upward movement close to the
392 wall of the fluidizing column. These resulted in a completed bed material turn over in addition
393 to the localized mixing caused by the bubbles movement. The surface of the expanded
394 material took a concave shape and the degree of curvature was affected by the distributor
395 plate angle. When using the convex distributor plate the upward movement was observed at
396 the center which also resulted in a complete bed material turn over. The surface of the
397 expanded bed material took a convex shape and the degree of curvature was also affected
398 by the distributor plate angle of convex. The flat distributor plate achieved good fluidization
399 and a uniform bed material expansion. Localized mixing caused by the upward movement of
400 the bubbles was clearly evident but no bed material turnover was observed.

401



402
403
404
405

Fig. 4. Bubble ejection stages.



406
407
408

Fig. 5. Bubble wake ejection [27].

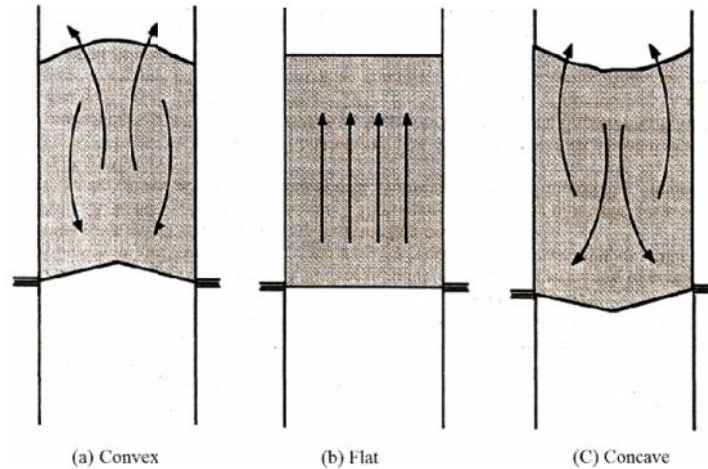


Fig. 6. Effect of distributor plate on the mixing pattern in a bubbling fluidized bed.

An analysis of variance was performed on the data as shown in Table 3. The effects of five variables (the sand particles size, the bed height, the distributor plate angle, the fluidizing velocity and the location of measurement) were highly significant at the 0.001 level. The analysis of variance also showed that the interactions between the various variables were highly significant at the 0.001 level.

In order to test the differences among the levels of each of the variables, Duncan's Multiple Range Test was carried out on the data. The results are shown in Table 4. The 10° convex and 10° concave were not significantly different from one another at the 0.5 level. Also, the 5° convex, 5° concave and flat plates were not significantly different from one another at the 0.5 level. The highest pressure drop was observed with the 10° convex. The two particle sizes were significantly different from one another at the 0.5 level and higher pressure drop was observed with the coarse particles. The three bed heights were significantly different from one another at the 0.5 level. The highest pressure drop was observed with the 2D bed height. The two fluidization velocities were significantly different from one another at the 0.5 level. The highest pressure drop was observed with the higher fluidization velocity of 1.75 U_{mf} . The first bed location above the plate (P_1) was significantly different from the other 3 locations (P_2 , P_3 and P_4) while these three locations were not significantly different from each other at the 0.05 level. The highest pressure drop was observed at the fourth location (P_4).

4.1. Effect of Plate Shape

The results showed that there were no significant differences between pressures from measurements across the five distributor plates taken when the bed was empty (i.e. no sand in the bed). However, with the fluidized bed a decrease in the angle of concave and an increase in the angle of convex decreased the pressure drop as shown in Figure 7. It appears that the shape (angle) of distributor plate affected the average bed height (Figure 8) thereby, affecting the pressure drop.

Svensson *et al.* [28] investigated the influence of air distributor design on the bubble rise velocity and frequency and pressure drop of circulating fluidized bed. They reported that pressure drop across the distributor was the only significant factor affecting the fluidizing regime. Increasing the pressure drop across the distributor lead to increases in bubble size and rise time resulting in reduced residence time.

448 **Table 3. Analysis of variance**

Source	DF	SS	MS	F	PR>F
TOTAL	359	502617.69			
MODEL	319	502427.47	1575.01	5299.15	0.001
DF	4	8036.32	2009.08	6759.60	0.001
PS	1	28754.70	28754.70	96745.93	0.001
BH	3	177328.37	591109.46	99999.99	0.001
FV	1	1224.92	1224.92	4124.27	0.001
XX	3	222981.51	74327.17	99999.00	0.001
DP*PS	4	3167.70	791.92	2664.45	0.001
DP*BH	12	178.79	14.90	50.13	0.001
DP*FV	4	111.25	27.91	93.57	0.001
DP*XX	12	109.80	9.15	30.79	0.001
PS*FV	1	616.00	616.00	2072.55	0.001
PS*XX	3	2.83	0.94	3.18	0.237
BH*FV	3	13.66	4.55	15.33	0.001
BH*XX	9	58312.73	6479.19	21799.41	0.001
FV*XX	3	5.00	1.66	5.61	0.001
DP*PS*BH	12	307.29	25.61	86.16	0.001
DP*PS*FV	4	12.97	3.24	10.91	0.001
DP*PS*XX	12	137.93	11.49	38.67	0.001
DP*BH*FV	12	100.31	8.36	28.12	0.001
DP*BH*XX	36	154.75	4.30	14.46	0.001
DP*FV*XX	3	2.02	0.67	2.27	0.001
DP*BH*FV	3	38.44	12.81	43.11	0.001
PS*BH*XX	9	30.98	3.44	11.58	0.001
BH*FV*XX	9	20.85	2.31	7.79	0.001
DP*PS*BH*FV	12	52.98	4.41	14.85	0.001
DP*BH*FV*XX	48	47.66	0.99	3.34	0.001
DP*PS*BH*XX	36	59.33	1.64	5.54	0.001
PS*BH*FV*XX	9	25.25	2.81	9.44	0.001
DP*PS*BH*FV*XX	48	77.81	1.62	5.45	0.001
ERROR	640	190.22	0.29		

449 $R^2 = 0.99$

450 $CV = 1.34\%$

451 $S =$ Particle size

452 $DP =$ Distributor plate

453 $BH =$ Bed Height

454 $FV =$ Fluidization velocity

455 $XX =$ Location of measurement

456

457 Sobrino et al. [29] conducted a study for measuring the distributor pressure drops in two
458 types of distributors including perforated plate and bubble cap distributor. The results
459 indicated that the pressure drop in the perforated plate distributor was due to the presence of
460 mesh which was sandwiched between the two plates. Whereas, the pressure drop across
461 bubble cap distributor is mainly due to the resistance to the flow in the entrance orifice.

462

463 **4.2. Effect of Sand Particle Size**

464 Greater values of pressure drop were obtained with the larger (536 mm) sand particle size
465 (coarse sand) as compared to those obtained with smaller (198 mm) sand particle size (fine
466 sand). On the average, pressure drops of 46.00 and 36.06 were obtained with the course
467 and fine sand, respectively. This is due to the difference in minimum fluidization velocity of

Table 4. Mean values of pressure drop as affected by the angle and shape of distributor plate, particle size, bed height, fluidization velocity and location of measurements.

Parameter	Number of observations	Mean pressure drop (KPa)	Grouping
Distributor plate angle			
10° convex	192	44.53	A
5° convex	192	40.47	B
Flat	192	39.53	B
5° concave	192	38.23	B
10° concave	192	36.47	A
Particle size (cm)			
0.0198	480	35.06	A
0.0536	480	46.00	B
Bed height (cm)			
0.5D	240	22.45	A
1.0D	240	34.30	B
1.5D	240	46.44	C
2.0D	240	58.92	D
Fluidization velocity			
1.50 U_{mf}	480	39.39	A
1.75 U_{mf}	480	41.66	B
Location			
P1	240	14.13	A
P2	240	49.32	B
P3	240	49.31	B
P4	240	49.34	B

Means with different letter are significantly different at 0.05 percent level

D = Inner diameter of the fluidizing column (cm)

U_{mf} = Minimum fluidizing velocity

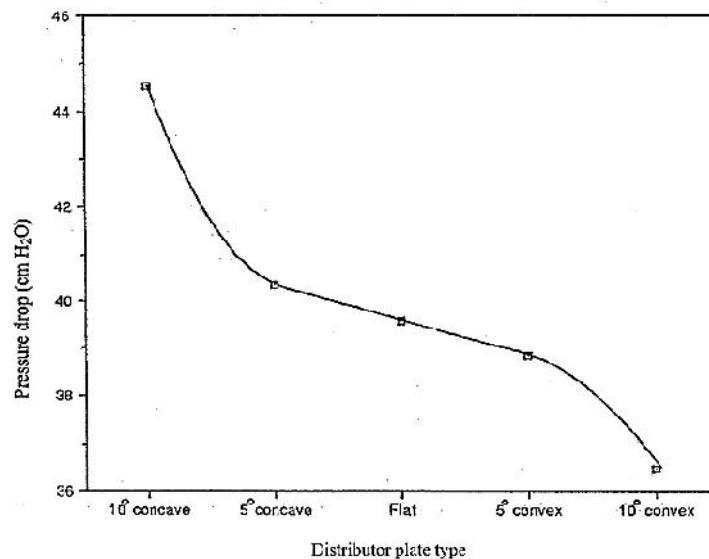


Fig. 7. Effect of distributor plate on pressure drop.

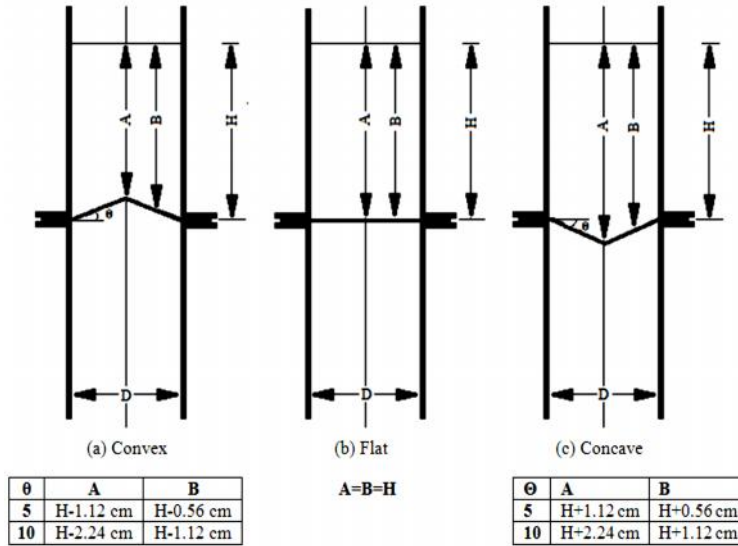


Fig. 8. Effect of distributor plate on the vertical transport of the tracer particles.

the fine sand (4.2 cm/s) from that of the coarse sand (26.0 cm/s) The pressure drop across a bubbling fluidized bed has a direct relationship with the minimum fluidization velocity of the particles in the bed. Particles with higher minimum fluidization velocities have greater pressure drop across the bed than particles having lower minimum fluidization velocities.

Guathier et al. [30] reported that particle size distributions have a strong influence on various fluidization characteristics including fluidization velocity and pressure drop. The study was carried out using four powders (narrow cut, binary mixture, Gaussian and wide cut) with different particle sizes ranging from 282.5 μm to 1800 μm . The authors found that a wide range of particle size has very different fluidization characteristics than powder with a narrow range of particle size. The results from the study indicated the increasing the particle diameter (size) increased the minimum fluidization velocity (U_{mf}) constantly and thereby increasing the total pressure drop across the bed.

Lin et al. [31] studied the effect of particle size on fluidization using four different types of powder including: a narrow powder, a binary mixture, a flat and Gaussian distribution powder. The results indicated that particles with higher fluidization velocities tend to segregate and increased the pressure drop across the bed. The results also showed that binary and flat powder had higher minimum fluidization velocities (U_{mf}) and segregated and increased the pressure drop across the bed, but narrow and Gaussian distribution powder had lower minimum fluidization velocities (U_{mf}) and were readily available for complete mixing.

4.3. Effect of Bed Height

An increase in the bed height increased the aspect ratio and as a result increased the pressure drop considerably. The relationship between the bed height and the aspect ratio was linear as shown in Figure 9. The value of the pressure drop varied from a low of 1.55 cm H_2O to a high of 7.09 cm H_2O , depending on the bed height and the distributor plate used. The pressure drop is a function of the weight of particles in the bed. Since the bed diameter is constant, an increase in bed height results in an increase in pressure drop. Similar findings were reported by Qureshi and Creasy [21].

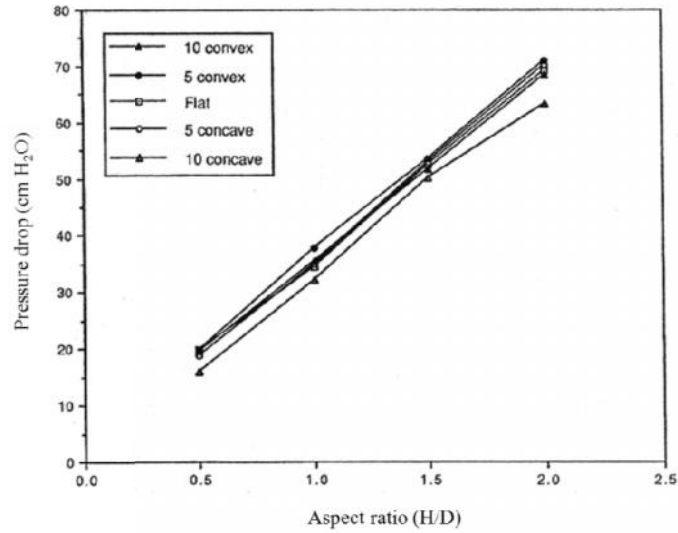


Fig. 9. Effect of aspect ratio on the pressure.

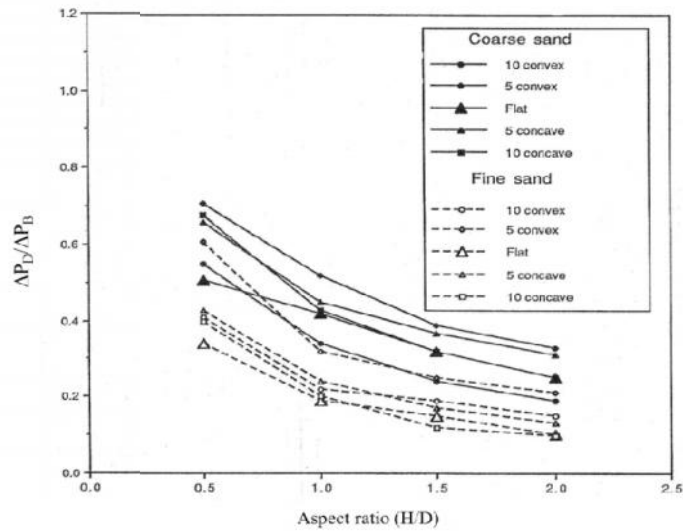


Fig. 10. Effect of aspect ratio on $\Delta P_D/\Delta P_B$.

The ratio of the pressure drop across the distributor plate to that across the bed (P_D/P_B) decreased with the increase in bed height. Figure 10 shows the variation of the ratio of the experimental pressure drop to the theoretical pressure drop (P_E/P_T) with the aspect ratio at $U/U_{mf}=1.75$ for the two sizes of sand particles used in the experiments. The pressure drop ratio decreases with the increase in bed aspect ratio for all distributor plates. Similar results were obtained with other fluidizing velocities. This agrees with the finding of Qureshi and Creasy [21] and Geldart and Baeyens [20].

Gelperin *et al.* [32] studied the variation in fluidization along an angled distributor plate and found the minimum fluidization velocity to vary from a minimum value at the site of the lowest bed height (highest point of distributor plate) to a maximum at the site of the greatest bed height (lowest point of the distributor plate). This variation created a gradient in the effective fluidization velocity and pressure experienced in different regions of the bed.

Taghipour et al. [18] reported that initially the bed height increased with bubble formation and then levelled off at the steady state. As a result, the bed overall pressure drop increased significantly at the beginning of fluidization and then fluctuated for about 3 s. Bi et al. [33] reported that bed oscillations were triggered by the disturbance in the gas flow due to which the bed height increased and settled after the disturbance was cut off. The authors suggested that pressure variations did not result from bed height variations instead it resulted due to the relaxation of layers of particles after they were displaced from their original positions.

Sathiyamoorthy and Horio [34] reported that pressure drop across a distributor is conventionally expressed as its ratio to bed pressure drop ($\Delta P_D/\Delta P_B$) and it is in the range of 0.1-0.4 for a uniform operation. The authors suggested that in a deep fluidized bed, the pressure drop is high and gas bypasses as large bubbles or slugs which affect heat and mass transfer rates. In a shallow the bed, the pressure drop is low as it has a low transport disengaging height and high a solid expansion ratio. The results from the study indicate that the bed pressure ratio ($\Delta P_D/\Delta P_B$) decreases with increases in aspect ratio and it increases with operating velocity.

4.4. Effect of Fluidization Velocity

The mean value of the pressure drop was increased when the fluidization velocity was increased from 1.25 to 1.50 U_{mf} as shown in Figure 11. Further increases in the pressure drop at high fluidizing velocity were very small. Generally, the pressure drop should not increase with increases in fluidizing velocity and the increase in pressure drop with increased fluidization velocity observed in this study was more or less within experimental accuracy for all distributor plates. This suggests that fluidizing velocities higher than 1.25 U_{mf} should be used in order to obtain good fluidization.

Menon and Durian [17] stated that there are three distinct regimes of behavior observed when velocity (U_s) is increased from zero. In the first regime, the values of velocity (U_s) are small at constant bed height. At this point, the pressure drops (ΔP) varies linearly with velocity (U_s) and depth as per Darcy's law. The bed has similar properties of a static heap of sand with a finite angle of repose at its surface. In the second regime, the velocity (U_s) attains minimum fluidization velocity (U_{mf}) at which the pressure drops (ΔP) is equal to the weight of the bed and the bed expands homogeneously. At this point, the medium behaves like a fluid and the angle of repose becomes zero and heavier particles sink while the lighter particles float. This is also called as uniformly fluidized state and no intensity fluctuations are seen at this state. The third state is the inhomogeneous state where the velocity (U_s) is above the threshold velocity leading the rising up as bubbles with a well-defined interface surrounded by a granular medium having a mushroom-cap shape. In this state, the bed expands with increase in velocity (U_s) with no change in pressure (ΔP). In this study, the pressure drop (ΔP) was studied across the fluidized bed at three different particle sizes (49, 96 and 194 μm) and velocity ranging from 0.1 to 10 cm/s. The results indicated that for all particle sizes when the velocity was increased from 0.1 to 10 cm/s the pressure drop increased linearly and the onset of bubbling began at a normalized pressure of 1 pgh.

Kawaguchi et al. [19] reported that when pressure drop increases the velocity of gas increases, but the velocity becomes constant at a certain point after which it exhibits overshoot. Inversely, when the gas velocity decreases, the pressure drop remains constant and then starts to decrease when the velocity becomes too low. The minimum fluidization velocity (U_{mf}) may be determined by the velocity at which the pressure starts to decrease. In this study the velocity of the gas was gradually increased to 4 m/s and then decreased gradually to 0 m/s and there were high fluctuations in the pressure due to bubbling and

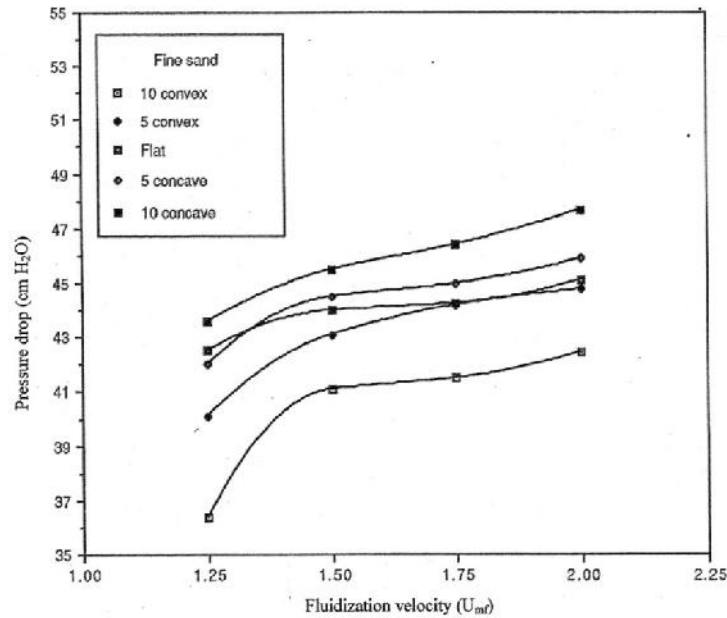


Fig. 11. Effect of fluidizing velocity on the pressure drop.

slagging and the results were averaged to obtain pressure drop values. The results indicated that the minimum fluidization velocity (U_{mf}) for the pressure was between 1.7-1.8 m/s. When the gas velocity reached 2.4 m/s the particles began to circulate in the whole region and the bubbles were periodically formed. It was also noticed that the circulation occurs only at the bottom and the particles at the top were not mixed well and the velocity at the corners was very low compared to those in the other regions. When the velocity was increased to 2.6 m/s there was consistent bubble formations and when the bubble erupts at the surface of the bed, the particles were mixed in the whole region.

4.5. Effect of Location of Pressure Probe

The pressure drop was measured across the distributor plate, at two locations in the freeboards and in the duct leading to the cyclone. There were significant differences among the other three locations in the freeboard and the duct as shown in Figure 12. The two points in the freeboard (P_2 and P_3) gave equal pressure drop readings. This is as expected since the flow conditions of the gas-solid stream were not much altered between the two locations. The finding that P_4 is equal to P_2 and P_3 was, however, not expected. Although, the velocity of the fluid increased at the exit due to the smaller area it was forced to pass through, the pressure drop did not decrease. The reason for this is probably that the fluidizing velocities used in these experiments were not great enough to cause a great change in fluid velocity at the contraction that could lead to detectable decrease in pressure drop.

Svoboda et al. [35] reported that location of pressure probe in the fluidized bed plays an important role. Their results indicated that the maximum amplitude occurred in the middle part of the fluidized bed and the amplitude tend to increase and then decrease with the distance from the distributor were also detected.

Bi et al.[33] studied the effect of port spacing and probe location across the fluidized bed. The authors reported that more extraneous pressure waves can be filtered out by reducing the spacing between the probes but the results indicated the velocity was not greatly affected by the port spacing within the test range. The flow of gas across the fluidized bed

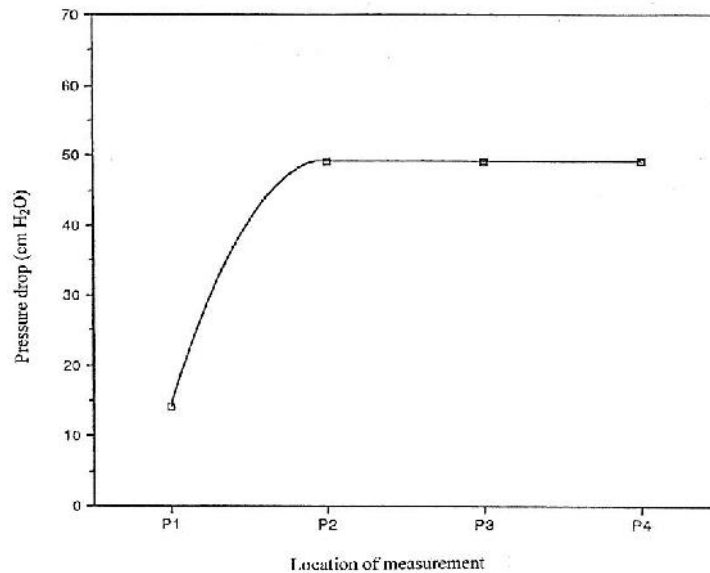


Fig. 12. Effect of location of measurement on pressure drop.

varied with axial location and different pressure peak points were obtained when the probe was moved to different locations.

6. CONCLUSIONS

A pilot scale fluidized bed system was used to study the effect of distributor plate shape and conical angle on the pressure drop. Five distributor plates (flat, concave with 5°, concave 10°, convex with 5° and convex with 10°) were used in the study. The system was tested at two levels of sand particle size (a fine sand of 198 μm and coarse sand of 536 μm), various bed heights (0.5 D, 1.0 D, 1.5 D and 2.0 D cm) and various fluidization velocities (1.25, 1.50, 1.75 and 2.00 U_{mf}). The pressure drop was affected by the shape and the conical angle of distributor plate, sand particle size and bed height. Less than theoretical values of the pressure drop were observed with the 10° concave distributor plate at lower fluidizing gas velocities for all bed heights. A decrease in the angle of convex and an increase in the angle of concave resulted in a decreased pressure drop. Greater values of pressure drop were obtained with larger sand particles than those obtained with small sand particles at all fluidizing velocities and bed heights. For all distributor plates, increasing the bed height increased the pressure drop but decreased the ratio of pressure drop across the distributor to the pressure drop across the bed ($\Delta P_D/\Delta P_B$). There was no variation in the pressure drop in the freeboard. Fluidizing gas velocities higher than 1.25 U_{mf} should be used to for a better fluidization, improved mixing and avoiding slugging of the bed.

REFERENCES

1. Pavia J, Pinho C, Figueiredo R. The Influence of the Distributor Plate on the Bottom Zone of a Fluidized Bed Approaching the Transition from Bubbling to Turbulent Fluidization. *Chem. Eng. Res. Des.* 2004, 82 (A 1): 25-33.
2. FAO. Energy for Agriculture. Food and Agriculture Organization of United Nations, Rome, Italy. 2013. Accessed on March 27, 2013. Available: <http://www.fao.org/docrep/003/X8O54E/x8O54eO5.htm>

- 649 3. Surisetty VR, Kozinski J, Dalai AK. Biomass, availability in Canada, and gasification: and
650 overview. *Biomass Conversion and Biorefinery*. 2012, 2: 73-85.
- 651 4. Goyal HB, Seal D, Saxena RC. Bio-fuels from thermochemical conversion of renewable
652 resources: A review. *Renewable and Sustainable Energy Reviews*. 2008, 12: 504-517.
- 653 5. Wood SM, Layzell DB. A Canadian Biomass Inventory: Feedstocks for a Bio-based
654 Economy. BIOCAP Canada Foundation, Kingston, Ontario, Canada, 2003.
- 655 6. Ergudenler A, Ghaly AE. Agglomeration of alumina sand in a fluidized bed straw gasified
656 at elevated temperatures. *Bioresour. Technol.* 1993, 48: 259-268.
- 657 7. Ergudenler A, Ghaly AE. Quality of gas produced from wheat straw in a dual distributor
658 fluidized bed gasifier. *Biomass and Bioenergy*. 1992, 3: 419-430.
- 659 8. Khan AA, DeJong W, Jansens PJ, Spliethoff H. Biomass combustion in fluidized bed
660 boilers: Potential problems and remedies. *Fuel Process. Technol.* 2009, 90: 21-50.
- 661 9. Rowe PN, Nienow AW. Particles mixing and segregation in gas fluidized beds: a review.
662 *Powder Technology*. 1976, 15: 141-147.
- 663 10. Mansaray KG, Ghaly AE. Air gasification of rice husk in a dual distributor type fluidized
664 bed reactor. *Energy Sources*. 1999, 2: 867-882.
- 665 11. Yoshida K, Kameyama H, Shimizu F. Mechanism of particle mixing and segregating in
666 gas fluidized beds. In *Fluidization*, Grace, J.R. and J.M. Matsen, (Eds.). Plenum Press, New
667 York, New York, USA, 1980.
- 668 12. Nemtsov DA, Zabaniotou A. Mathematical modelling and simulation approaches of
669 agricultural residues air gasification in a bubbling fluidized bed reactor. *Chem. Eng. J.* 2008,
670 143: 10-31.
- 671 13. Ghaly AE, MacDonald KN. Mixing patterns and residence time determination in a
672 bubbling fluidized bed system. *American Journal of Engineering and Applied Science*. 2012,
673 5(2): 170-183.
- 674 14. Bonniol F, Sierra C, Occelli R, Tadrist, L. Similarity in dense gas-solid fluidized bed,
675 influence of the distributor and the air-plenum. *Powder Technology*. 2009, 189: 14-24.
- 676 15. Sundaresan S. Instabilities in fluidized beds. *Annual Review of Fluid Mechanics*. 2003,
677 35: 63-88.
- 678 16. Basu, P. *Combustion and Gasification in Fluidized Beds*. Taylor and Francis Group, LLC,
679 Florence, Kentucky, USA, 2006.
- 680 17. Menon N, Durian DJ. Particle motions in a gas-fluidized bed of sand. *Phys. Rev. Lett.*
681 1997, 79(18): 3407-3410.
- 682 18. Taghipour F, Ellis N, Wong C. Experimental and computational study of a gas-solid
683 fluidized bed hydrodynamics. *Chem. Eng. Sci.* 2005, 60: 6857-6867.
- 684 19. Kawaguchi T, Tanaka T, Tsuji Y. Numerical simulation of two-dimensional fluidized bed
685 using the discrete element method (comparison between the two and three dimensional
686 models). *Powder Technology*. 1998, 96: 129-138.
- 687 20. Geldart D, Baeyens J. The Design of Gas Distributors for Gas Fluidized Beds. *Power*
688 *Technology*. 1985, 42: 67-78.
- 689 21. Qureshi AE, Creasy DE. Fluidized Bed Gas Distributors. *Power Technology*. 1979, 20:
690 47-52.
- 691 22. Clift R. *Hydrodynamics of Bubbling Fluidized Beds in Gas Fluidization Technology* (Ed.
692 D. Geldart). John Wiley and Sons, New York, New York, USA, 1986.
- 693 23. Geldart D. Single Particles, Fixed and Quiescent Beds. In: *Gas Fluidization Technology*,
694 (Ed. D. Geldart), John Wiley & Sons, New York, New York, USA, 1986.
- 695 24. Kunii D, Levenspiel, O. *Fluidization Engineering*. Kreiger Publishing Company, New
696 York, USA, 1977.
- 697 25. Ergudenler A, Ghaly AE, Hamdullahpur F, Al-Taweel AM. Mathematical modelling of a
698 fluidized bed straw gasifier: Part II- Model sensitivity. *Energy Sources*. 1997, 19: 1085-1098.
- 699 26. Gibilaro LG. *Fluidization Dynamics*. Elsevier Butter Worth-Heinemann. Waltham,
700 Massachusetts, U.S.A., 2001.

701 27. Muller CR, Davidson JF, Dennis JS, Hayhurst AN. A study of the motion and eruption of
 702 a bubble at the surface of a two-dimensional fluidized bed using Particle Image Velocimetry
 703 (PIV). *Ind. Eng. Chem. Res.* 2007, 46: 1642-1652.
 704 28. Svensson A, Johnsson F, Leckner B. Fluidization regimes in non-slugging fluidized beds:
 705 The influence of pressure drop across the air distributor. *Powder Technology.* 1996, 86: 299-
 706 312.
 707 29. Sobrino C, Ellis N, de Vega M. Distributor effects near the bottom region of turbulent
 708 fluidized beds. *Powder Technology.* 2009, 189: 25-33.
 709 30. Gauthier D, Zerguerras S, Flamant G. Influence of the particle size distribution of
 710 powders on the velocities of minimum and complete fluidization. *Chem. Eng. J.* 1999, 74:
 711 181-196.
 712 31. Lin CL, Wey MY, You SD. The effect of particle size distribution on minimum fluidization
 713 velocity at high temperature. *Powder Technology.* 2002, 126: 297-301.
 714 32. Gelperin NI, Ainshtein VG, Pogorelaya LD, Lyamkin VA, Terekhow NI. Limits of stable
 715 fluidization regimes in vessel with inclined gas distributor grid. *Chem. Technol. Fuels Oils.*
 716 1982,18: 20-24.
 717 33. Bi HT, Grace JR, Zhu J. Propagation of pressure waves and forced oscillations in gas
 718 solid fluidized beds and their influence on diagnostics of local hydrodynamics. *Powder*
 719 *Technology.* 1995, 82: 239-253.
 720 34. Sathiyamoorthy D, Horio M. On the influence of aspect ratio and distributor in gas
 721 fluidized beds. *Chem. Eng. J.* 2003, 93: 151-161.
 722 35. Svoboda K, Cermak J, Hartman M, Drahos J, Selucky K. Pressure fluctuations in gas-
 723 fluidized beds at elevated temperatures. *Industrial and Engineering Chemical Process.* 1983,
 724 22(3): 514-520.
 725
 726
 727